iScience, Volume *24*

Supplemental information

Interactions between fungal hyaluronic acid and host CD44 promote internalization by recruiting host autophagy proteins to forming phagosomes

Shengli Ding, Jing Yang, Xuehuan Feng, Aseem Pandey, Rola Barhoumi, Dongmei Zhang, Samantha L. Bell, Yue Liu, Luciana Fachini da Costa, Allison Rice-Ficht, Robert O. Watson, Kristin L. Patrick, Qing-Ming Qin, Thomas A. Ficht, and Paul de Figueiredo

Transparent Methods

Key resources table

REAGENT or RESOURCE	SOURCE	IDENTIFIER
Antibodies		
Mouse anti-*C. neoformans* 18B7	Dr. Arturo Casadevall, (Albert Einstein College of Medicine of Yeshiva University, NY, USA)	N/A
CD44 Antibody [IM7]	GeneTex, Inc. (North America)	Cat. #: GTX80086
Mouse anti-HCAM(CD44)	Santa Cruz Biotechnology, Inc. (Dallas, TX USA)	Cat. #: sc-7297
anti-pCaMKKβ	Cell Signaling Technology, Inc. (Danver, MA USA)	Cat. #:16737S
anti-CaMKKα	Santa Cruz Biotechnology, Inc. (Dallas, TX USA)	Cat. #: sc-11370/17827
anti-CaMKKβ	Santa Cruz Biotechnology, Inc. (Dallas, TX USA)	Cat. #: sc-271674
Rabbit anti-pAMPKα (Thr 172)	Cell Signaling Technology, Inc. (Danver, MA USA)	Cat. #: 2535
Rabbit anti-AMPKα	Cell Signaling Technology, Inc. (Danver, MA USA)	Cat. #: 5831
Rabbit-anti pULK1 (Ser 555)	Cell Signaling Technology, Inc. (Danver, MA USA)	Cat. #: 5869
Rabbit anti-ULK1	Santa Cruz Biotechnology, Inc. (Dallas, TX USA)	Cat. #: sc-33182
Rabbit anti-LC3	Santa Cruz Biotechnology, Inc. (Dallas, TX USA)	Cat. #: sc-134226
Rabbit anti-GAPDH	Santa Cruz Biotechnology, Inc. (Dallas, TX USA)	Cat. #: sc-25778
Atg9A (D4O9D) Rabbit mAb	Cell Signaling Technology, Inc. (Danver, MA USA)	Cat. #: 13509S
Rabbit anti-ATG13	Sigma-Aldrich, Inc. (St. Louis, MO USA)	Cat. #: SAB4200100
Atg13 (E1Y9V) Rabbit mAb	Cell Signaling Technology, Inc. (Danver, MA USA)	Cat. #: 13468S
Rabbit anti-FIP200	Proteintech Group, Inc. (Rosemont, IL USA)	Cat. #: 17250-1-AP
Rabbit anti-AMPKβ	Novus Biologicals, Inc. (Littleton, CO USA)	Cat. #: NBP1-87487
Rabbit anti-pLKB1 (Ser428)	Abcam, Inc. (Cambridge, MA USA)	Cat. #: Ab63473
Rabbit anti-pAMPK (Thr172)-PE	BIOSS, Inc. (Woburn, MA USA).	Cat. #: BS-4002RP
Rabbit anti-pATG1 (Ser556)-PE	BIOSS, Inc. (Woburn, MA USA)	Cat. #: ABIN746733
Fungal, Bacterial and Virus Strains		
C. neoformans strain H99	Dr. Xiaorong Lin (Texas A&M University, College Station, TX)	N/A
C. neoformans strain AI100-dsRed	Dr. Xiaorong Lin (Texas A&M University, College Station, TX)	N/A
C. neoformans strain cap59	Dr. Xiaorong Lin (Texas A&M University, College Station, TX)	N/A
C. neoformans strain C177	Dr. Jong, A. (University of California, Los Angeles, CA, USA)	N/A
C. neoformans strain *cps1*Δ	Dr. Jong, A. (University of California, Los Angeles, CA, USA)	N/A
C. neoformans strain C588	Dr. Jong, A. (University of California, Los Angeles, CA, USA)	N/A
Chemicals, Peptides, and Recombinant Proteins		
STO-609	Sigma-Aldrich, Inc. (St. Louis, MO USA)	Cat. #: S1318-5MG
BAPTA-AM	Sigma-Aldrich, Inc. (St. Louis, MO USA)	Cat. #: A1076-25MG
KN62	Sigma-Aldrich, Inc. (St. Louis, MO USA)	Cat. #: I2142-1MG
RIPA buffer	G-Biosciences (San Diego, CA USA)	Cat. #: 786-489
Phosphatase inhibitor cocktail 2	Sigma-Aldrich, Inc. (St. Louis, MO USA)	Cat. #: P5726
Phosphatase inhibitor cocktail 3	Sigma-Aldrich, Inc. (St. Louis, MO USA)	Cat. #: P0044
Amino-polystyrene Particles	Spherotech, Inc. (Lake Forest, IL, USA)	Cat #: AP-10-10
Hyaluronic acid	Santa Cruz Biotechnology, Inc. (Dallas, TX USA)	Cat #: sc-337865
EDC hydrochloride	Santa Cruz Biotechnology, Inc. (Dallas, TX USA)	CAS #: 25952-53-8

pENTR4-eGFP-C1 entry vector	Addgene (Cambridge, MA, USA)	Plasmid #17396
pLenti-PGK-Neo destination vector	Addgene (Cambridge, MA, USA)	Plasmid #19067
psPAX2	Addgene (Cambridge, MA, USA)	Plasmids #12260
pMD2G/VSV-G	Addgene (Cambridge, MA, USA)	Plasmids #12259
G418	Invivogen (San Diego, CA, USA)	Cat #: NC9227938
Lipofectamine™ 2000	Invitrogen (Carlsbad, CA, USA)	Cat #: 11668027
Critical Commercial Assays		
Phagocytosis Assay Kit (IgG FITC)	Cayman Chemical, Inc. (Ann Arbor, MI USA)	Cat. #: 500290
Fe-NTA column	Thermo Fischer Scientific (Waltham, MA USA)	Cat. #: 88300
Pierce ECL Plus chemiluminescence kit	Thermo Fischer Scientific (Waltham, MA USA)	Cat. #: 32132X3
Experimental Models: Cell Lines		
RAW264.7 cells	ATCC (Manassas, VA USA)	TIB-71
J774A.1 cells	ATCC (Manassas, VA USA)	TIB-67
GFP-Gal8 (RAW264.7 macrophages)	This work	NA
GFP-LC3 (RAW macrophages)	Dr. Douglas Green (St. Jude Children's Research Hospital, Pittburgh, PA USA)	NA
B6J2 cells	Dr. J. Suttles (University of Louisville, Louisville, KY USA)	(Sag et al., 2008)
B6J2 cells (AMPKα-DN)	Dr. J. Suttles (University of Louisville, Louisville, KY USA)	(Sag et al., 2008)
Experimental Models: Organisms/Strains		
C57BL/6 wild-type (WT) mice	Jackson Laboratories, Inc. (Bar Harbor, ME USA)	Stock No: 000664
CD44-KO mice (B6.129 (Cg)-*Cd44*^{tm1Hbg}/J)	Jackson Laboratories, Inc. (Bar Harbor, ME USA)	Stock #: 005085

Experimental model details

Bone marrow-derived macrophage harvest and cultivation

Bone marrow cells were collected from the femurs of littermate control and CD44 KO mice, and cultivated in L929-cell conditioned media [DMEM medium containing 20% L929 cell supernatant, supplemented with 10% (v/v) FCS, penicillin (100 U/ml), and streptomycin (100 U/ml)]. After 3 days of culture, non-adherent precursors were washed away and the retained cells were propagated in fresh L929-cell conditioned media for another 4 days. For experimentation, BMDMs were split in 24-well plates at a density of 2.5×10^5 cells per well in L929-cell conditioned media and cultured at 37°C with 5% CO_2 overnight before use.

Method Details

Cryptococcus Strains and Infection, cell Culture and colony formation unit (CFU) assay

Yeast forms of Cn cells were cultured on YPD (Difco™) agar plates and maintained on the plates for 4 to 5 days prior to experimentation. Mammalian cell lines were routinely incubated in DMEM supplemented with 10% FBS in a 5% CO_2 atmosphere at 37°C. Preparation of cryptococcal and host cells for infection as well as CFU assays that measured internalized Cn cells were performed as previously described (Qin et al., 2011; Pandey et al., 2017). For CFU assay, host cells were infected with antibody-opsonized Cn cells at a multiplicity of infection (MOI) of 1 or 10 for 3 hrs; for immunofluorescence microscopy analysis, host cells were infected with antibody-opsonized or non-opsonized Cn cells with an MOI of 5 (unless otherwise indicated) for 1 to 3 h. At the indicated h.p.i., the infected cells were harvested for CFU assays or fixed and performed immunofluorescence microscopy assays (see below). To heat-kill Cn for use in immunofluorescence microscopy assays, Cn cells were heat inactivated as previously described (Wang et al., 2019). Briefly, the suspension of Cn cells (2.5×10^8 Cn cells/ml) was aliquoted into 2.0 ml Eppendorf tubes and heated on a hot plate at 75°C for 90 min. The death of the Cn cells was confirmed by plating the heat-treated cell suspension on YPD agar plates.

Immunofluorescence microscopy assays for Cn phagocytosis

Mammalian host cells were first cultivated on 12 mm glass coverslips (Fisherbrand) on the bottom of 24-well plates (Falcon) for 12-16 h before infection. Next, the host cells were infected with the tested Cn cells and incubated at 37°C in a 5% CO_2 atmosphere. At the indicated time points post-infection, culture media was removed and the infected host cells were washed 6 to 8 times with PBS (pH 7.4) before being fixed with 3.7% formaldehyde. The fixed cells (at room temperature for 1 to 2 hrs) were then processed Cn phagocytosis assays using antibody (18B7) directed against Cn as previous described (Qin et al., 2011; Pandey et al., 2017) without adding Triton X-100 to the staining buffer. The numbers of internalized (unstained) and extracellular (stained) Cn cells were then quantified and plotted. Images represent a representative image from triplicate replicates, with 100 fields imaged per replicate.

Drug/compound treatments

Murine macrophage J774.A1 or RAW264.7 cells were overnight cultured in 48 well plates and then coincubated with assorted pharmacological compounds, including KN62 (5 μM), STO-609 (5 μM) or BAPTA-AM (7.5 μM) for 2 h. Cells treated with the solvent dimethyl sulfoxide (DMSO) for these compounds served as controls. The media containing the compounds was then

removed. For CFU assays, the drug-treated cells were extensively washed with fresh medium and then infected with Cn cells. At 3 h.p.i., the infected cells were lysed and performed CFU assay as previously described (Qin et al., 2011; Pandey et al., 2017). For western blots, the compound-treated cells were washed 3 times with cold 1 × PBS, pH7.4, lysed and performed immunoblotting assay as previously describe (Pandey et al., 2017).

Lentivirus-mediated depletion of host proteins

The pSuperRetro retrovirial vector system (OligoEngine, Inc.) was used to knockdown target gene expression in murine cells according to the manufacturer's instructions. The oligonucleotides used for shRNA construction to knockdown the expression of mouse genes and the accompanying references are listed in **Table S1**. Transfection was performed in 6-well plates containing 1.5×10^5 RAW264.7 or B6J2 cells. Clones with the insert stably integrated were selected with puromycin. Western blot was performed to validate the depletion of the targeted proteins. All Westerns were performed in triplicate and representative findings are shown.

Generation of GFP-tagged Gal8 RAW264.7 cells

The GFP-galectin-8 expression construct was made by first cloning the cDNA sequence of *Lgals8* (from RAW 264.7 cells) into the pENTR4-eGFP-C1 entry vector (Campeau et al., 2009), resulting in a fusion of eGFP on the N-terminus of galectin-8. This construct was fully Sanger sequenced (Eton Biosceinces, San Diego, CA) to verify the fusion protein was in-frame and error-free. GFP-Gal8 was then Gateway cloned with LR Clonase (Invitrogen) into the pLenti-PGK-Neo destination vector (Campeau et al., 2009). Lenti-X 293T cells (Takara Bio) were co-transfected with pLenti-GFP-Gal8 and the packaging plasmids psPAX2 and pMD2G/VSV-G (Addgene Plasmids #12259-60) to produce lentiviral particles. RAW 264.7 cells were transduced with GFP-Gal8 lentivirus for two consecutive days plus 1:1000 Lipofectamine 2000 (Invitrogen) and selected for 5 days with 750 μg/ml G418 (Invivogen). Expression of GFP-Gal8 was confirmed by Western blot analysis and fluorescence microscopy.

Confocal microscopy assays

Host cells were infected with live or heat killed, opsonized or unopsonized capsular or acapsular strains of Cn. At the indicated times post-infection, host cells were fixed for confocal immunofluorescence microscopy analysis using antibodies directed against the indicated host

proteins. Immunofluorescence microscopy staining and imaging methods (Qin et al., 2008; Qin et al., 2011; Pandey et al., 2017; Pandey et al., 2018) were used to determine the subcellular localization of host AIC components in infected host cells. Samples were observed on a laser scanning confocal microscope or on a confocal fluorescence microscope (ECLIPSE Ti, Nikon). Confocal images (1,024 × 1,024 pixels) were acquired and processed with NIS elements AR 3.0 software (Nikon) and assembled with Adobe Photoshop CC 2019 (Adobe Systems, CA, USA). Digital image analysis and quantification was performed as previously described (Qin et al., 2011). Findings from our subcellular localization analyses were not an artifact of secondary antibody cross reactivity with host or pathogen components because negligible fluorescence signal was observed when infected cells were stained with secondary antibodies alone, or the pathogen alone was stained with the antibodies used in the experiments (**Figure S5G**).

Protein pull-down assays

For protein pull-down assay with HA-coated or naked beads, spherical amino polysterene beads (size: 1.0-1.4 µm, Spherotech Inc, IL, USA) were covalently coupled using EDC [*N*-Ethyl-*N'*-(3-dimethylaminopropyl)carbodiimide hydrochloride] to hyaluronic acid (HA) (Santa Cruz Biotec.) as per the manufacturer's (Spherotech) instruction. Briefly, 200 µl of 0.05 M sodium acetate buffer (pH 5.0), 2 mg of HA, 2 ml of 5% w/v Amino particles and 20 mg of EDC were mixed in a glass centrifuge tube. The contents were vortexed and incubated for 2 hrs at ambient temperature on a rotary mixer. Following incubation, the tube was centrifuged at 3000 × g for 15 minutes and supernatant was carefully discarded. The pellet was washed twice in 1 × PBS and resuspended in 2 ml of 1 × PBS to obtain 5% w/v suspension of HA coated beads. RAW 264.7 cells (3×10^5) were washed with 1 × PBS. Next, a bead incubation solution containing 5 µl of HA-coated or naked beads in 200 µl of PBS was added to the washed cells. The cells were centrifuged for 10 min at 1500 RPM and then incubated in a humidified incubator containing 5% CO_2 for 2 hrs. The treated cells were washed 2-4 times with ice-cold 1 × PBS and lysed in 80 µl RIPA buffer supplemented with a cocktail of protease and phosphatase inhibitors. Beads were separated from the lysate by high-speed centrifugation at 4°C. The separated beads were washed 3 times with RIPA buffer and finally resuspended in 80 µl RIPA buffer and 20 µl of 5 × sample buffer (Thermo Scientific) and boiled for 5 mins. Samples were finally resolved by SDS-PAGE and subjected to western blot analysis.

For testing host CD44 physical interactions with AIC components during Cn infection, BMDMs were infected with H99 at an MOI of 10. At the indicated (0, 1, 2, 3) h.p.i., Cn infected cells were lysed. We then performed protein pull-down assays with CD44 as an input. The assays were performed using the Pierce Co-Immunoprecipitation (Co-IP) Kit (Thermo Scientific, USA) according to the manufacturer's instructions.

Immunoblotting analysis

Preparation of protein samples and western blot analysis were performed as described previously (Qin et al., 2011; Pandey et al., 2017; Pandey et al., 2018). Blot densitometry was performed using the ImageJ (http://rsbweb.nih.gov/ij/) software package. All Westerns were performed in triplicate and representative findings are shown.

Intracellular Ca^{2+} measurements

Measurement of intracellular Ca^{2+} levels of host cells infected with Cn cells, HA-treated and control cells were performed as the method previously described (Barhoumi et al., 2007). Briefly, cells were loaded for 1 h with 3.0 μM fluo4-AM at 37 °C in serum- and phenol red-free medium and then washed with the same medium. Fluo4-AM is a visible wavelength probe which exhibits about a 40 fold enhancement of fluorescence intensity upon Ca^{2+} binding (Gee et al., 2000). Fluo4-AM fluorescence was generated in the cells by argon laser excitation at 488 nm and fluorescence emission between 500 and 550 nm was monitored. Images were collected with Zeiss LSM 510 confocal microscope using a 63× objective/1.4 oil. Images presented have dimensions of 50 μm × 50 μm.

Quantification and statistical analysis

The quantitative data presented in this work represent the mean ± standard error of mean (SEM) from at least three independent experiments. To easily compare results from independent experiments, the data from controls, such as protein expression level, blot densitometry, CFU, intracellular Cn number, etc., were normalized as 1 or 100%. The significance of the data was assessed using the Student's *t*-test to assess statistical significance between two experimental groups or a one-way ANOVA test to evaluate the statistical differences of multiple comparisons of the data sets.

Supplemental Information

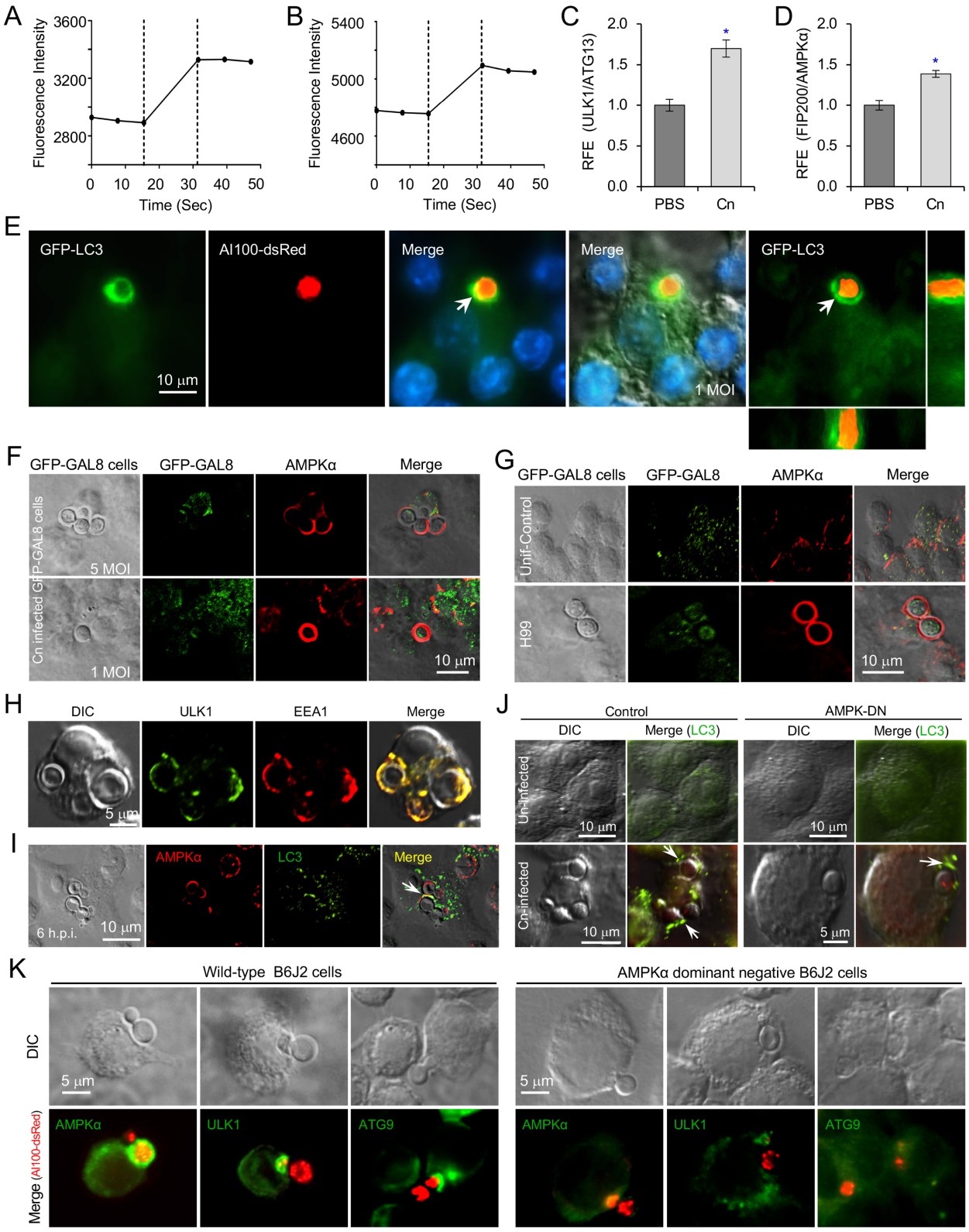

Figure S1. Recruitment of AIC components, but not galectin 8, to nascent phagosomes during *Cryptococcus neoformans* (Cn) internalization (Related to Figure 1).

The indicated host cells were infected with Cn cells at an MOI of 5. At 3 hrs post infection (h.p.i.), the infected host cells were fixed (3.7% formaldehyde in 1×PBS at room temperature for ~2 hrs) and subjected to Forster Resonance Energy Transfer (FRET) imaging microscopy (Irving et al., 2014; Wolf et al., 2013) or confocal immunofluorescence microscopy assays with the indicated antibodies.

(A, B) Fluorescence intensity of ULK1 and ATG13 (A) or FIP200 and AMPKα (B) during Cn internalization.

(C, D) Interactions between host ULK1 and ATG13 (C) or FIP200 and AMPKα (D) during recruitment to Cn-containing vacuoles (CnCVs) in RAW264.7 macrophages. The infected host cells were determined using FRET analysis. RFE: relative FRET-efficiency (between the FRET-pairs in the parentheses). The FRET-efficiency of Cn infected cells was compared to PBS control (normalized as 1). Data represent the means ± standard error of mean (SEM) from at least three independent experiments. *: significance at $p < 0.05$.

(E) Recruitment of host LC3 to nascent CnCVs during Cn (unopsonized) internalization.

(F, G) Host galectin 8 is not recruited to nascent phagosomes containing Cn cells during Cn internalization by host cells expressing GFP-galectin 8 (F) or cells supplemented with UBEI-41, a cell permeable inhibitor of ubiquitin-activating enzyme E1 (G).

(H) Colocalization of the host early endosomal marker EEA1 with AIC component ULK1 surrounding nascent CnCVs.

(I) Recruitment of host AMPKα and LC3 to nascent phagosomes containing Cn cells in infected bone marrow derived macrophages (BMDMs).

(J) Recruitment of host LC3 to nascent phagosomes containing Cn cells in infected or uninfected B6J2 macrophages expressing a dominant negative variant of AMPKα (AMPK-DN) or control.

(K) Less recruitment of host AMPKα and AIC component ULK1 or ATG9 to nascent CnCVs in B6J2 macrophages expressing an AMPK-DN variant during Cn internalization.

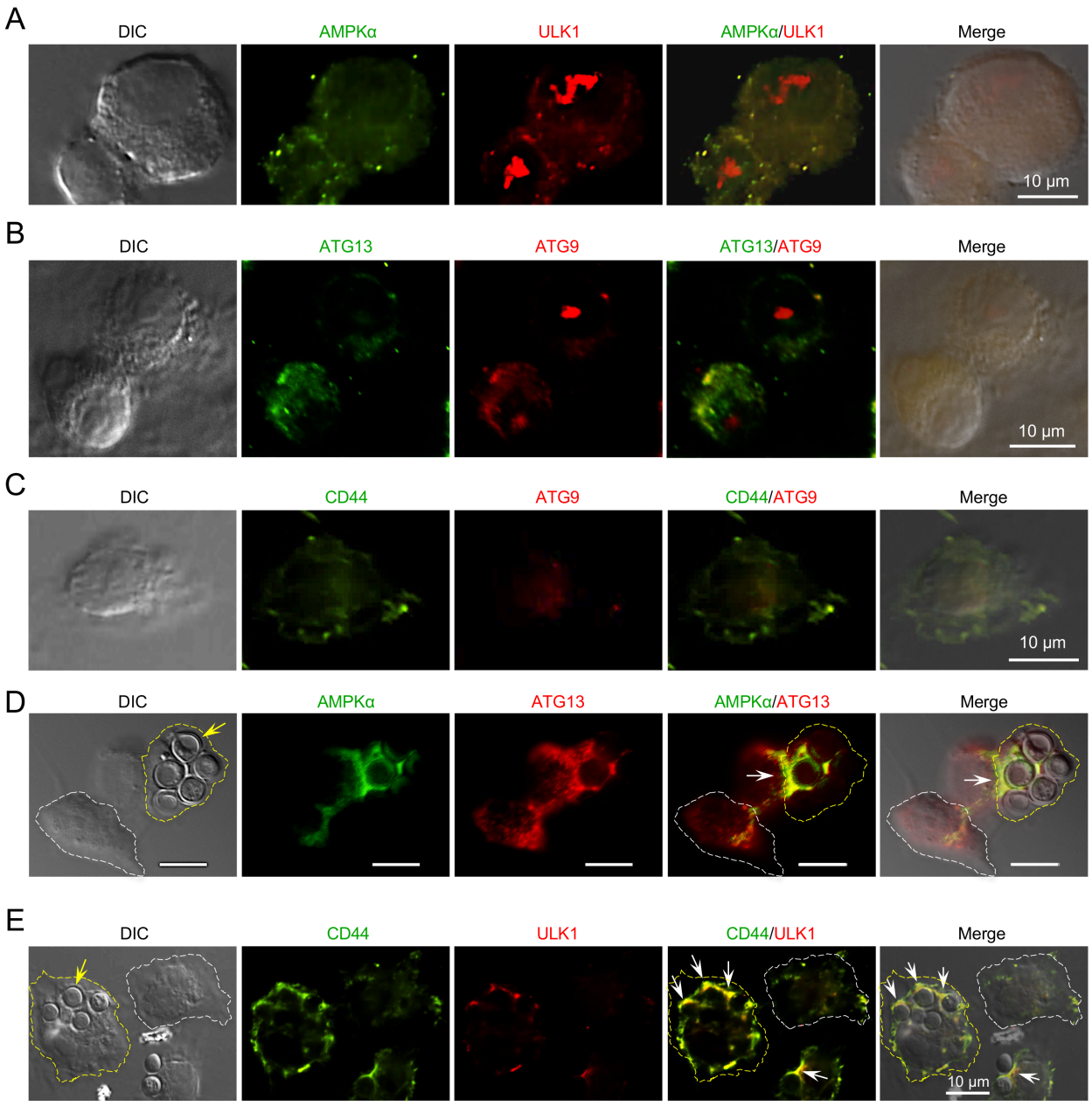

Figure S2. Expression and localization of the indicated host proteins in cells with or lacking Cn cells (Related to Figures 1, 2 and 3).

(A-C) Expression and localization of AMPKα and ULK1 (A), ATG9 and ATG13 (B), CD44 and ATG13 (C) in uninfected host cells.

(D, E) Comparison of the expression and localization of AMPKα and ATG13 (D, related to Figure 1A) or CD44 and ULK1 (E, related to Figure 3D) in Cn infected host cells containing or lacking Cn cells (bounded with yellow and white dash lines, respectively). Bars: 10 μm. Yellow arrows: Cn cells; white arrows: colocalization of the indicated proteins.

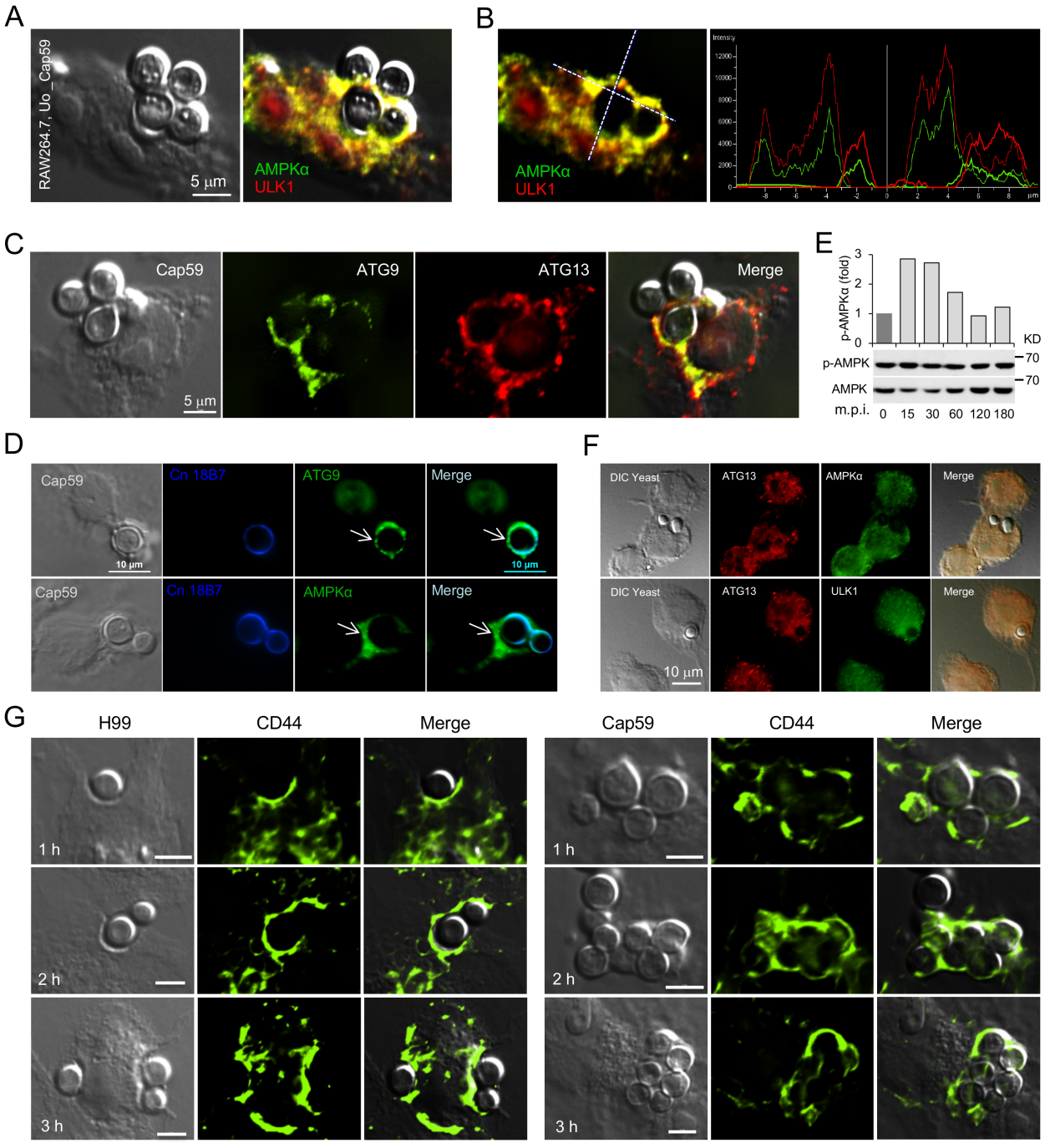
A
RAW264.7, Uo_Cap59
5 μm
AMPKα
ULK1
B
AMPKα
ULK1
Intensity
μm
C
Cap59
5 μm
ATG9
ATG13
Merge
E
p-AMPKα (fold)
KD
p-AMPK
AMPK
70
70
m.p.i.
0 15 30 60 120 180
D
Cap59
Cn 18B7
ATG9
Merge
10 μm
Cap59
Cn 18B7
AMPKα
Merge
F
DIC Yeast
ATG13
AMPKα
Merge
DIC Yeast
ATG13
ULK1
Merge
10 μm
G
H99
CD44
Merge
Cap59
CD44
Merge
1 h
2 h
3 h
1 h
2 h
3 h

Figure S3. Recruitment of host AIC components and CD44 to forming or nascent CnCVs during Cn internalization (Related to Figures 1, 2 and 3).

(A) Recruitment of AMPKα and AIC components ULK1 to nascent CnCVs. Uo_cap59: Unopsozied cap59.

(B) The fluorescence intensity profile of AMPKα and ULK1 along the two crossed white lines (left panel).

(C) Colocalization of ATG9 with ATG13 in the vicinities of CnCvs.

(D) Colocalization of host AMPKα or ATG9 with cryptococcal glucuronoxylomannan (GXM)-specific monoclonal antibody 18B7.

(E) Activation of host AMPKα by heat-killed (HK) Cn cells (cap 59) during phagocytosis. Representative results from one of three independent experiments are shown.

(F) Recruitment of AIC components and AMPKα to nascent phagosomes is minimally detected during phagocytosis of yeast (*Saccharomyces cerevisiae*) cells by host cells.

(G) Recruitment of CD44 during a time course (3 hr) of Cn internalization. Bars: 5 μm.

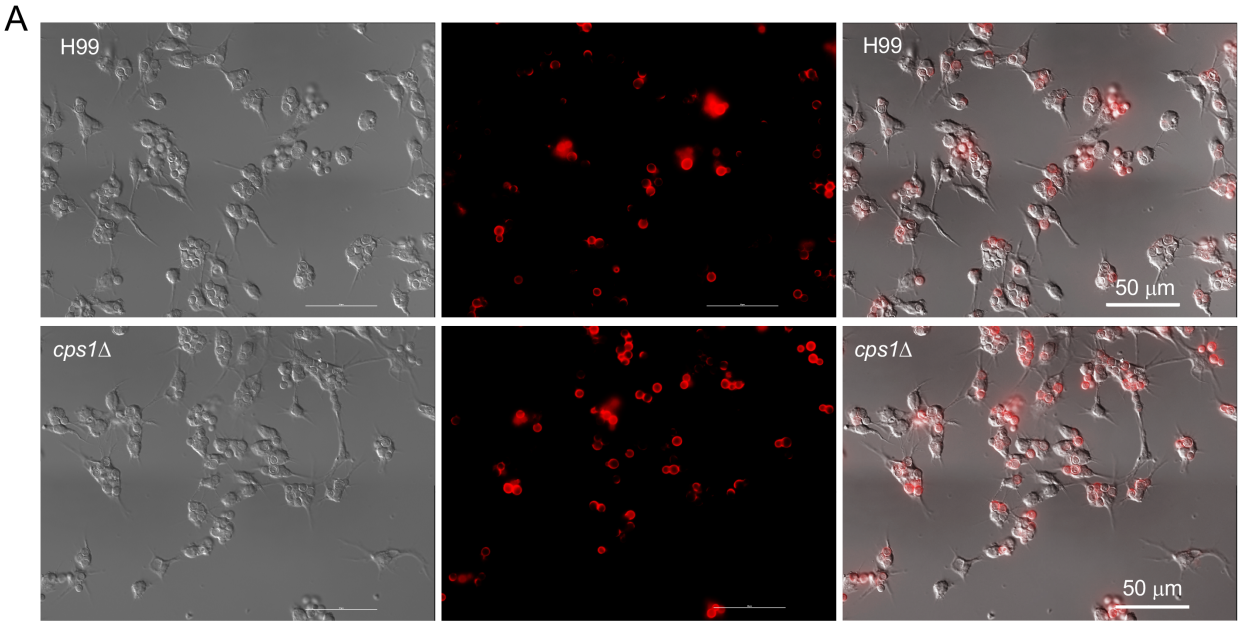
A
H99
H99
50 μm
cps1Δ
cps1Δ
50 μm

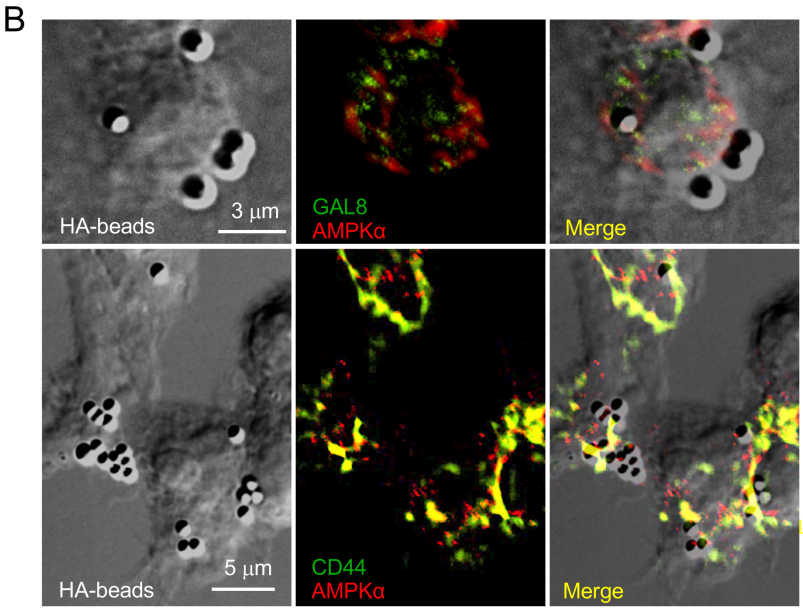
B
HA-beads
3 μm
GAL8
AMPKα
Merge
HA-beads
5 μm
CD44
AMPKα
Merge

Figure S4. Fungal hyaluronic acid (HA) is required for Cn internalization (Related to Figure 3).

(A) Disruption of Cn *cps1* impairs internalization of the fungal pathogen (related to Figure 3B-C). BMDMs were infected with the indicated Cn cells at an MOI of 10. At 3 h.p.i., the infected cells were fixed and then subjected to non-permeable immunofluorescence staining (Pandey et al., 2017) with Cn GXM-specific monoclonal antibody 18B7. Cn cells with red fluorescence represent incompletely internalized or extracellular Cn cells.

(B) Recruitment of CD44, not galectin 8, to the forming or nascent phagosomes associated with HA-coated beads. Upper panel: localization of galectin 8 (GAL8) and AMPKα in cells incubated with HA-coated beads. Lower panel: colocalization of CD44 and AMPKα to the forming or nascent phagosomes related to HA-coated beads.

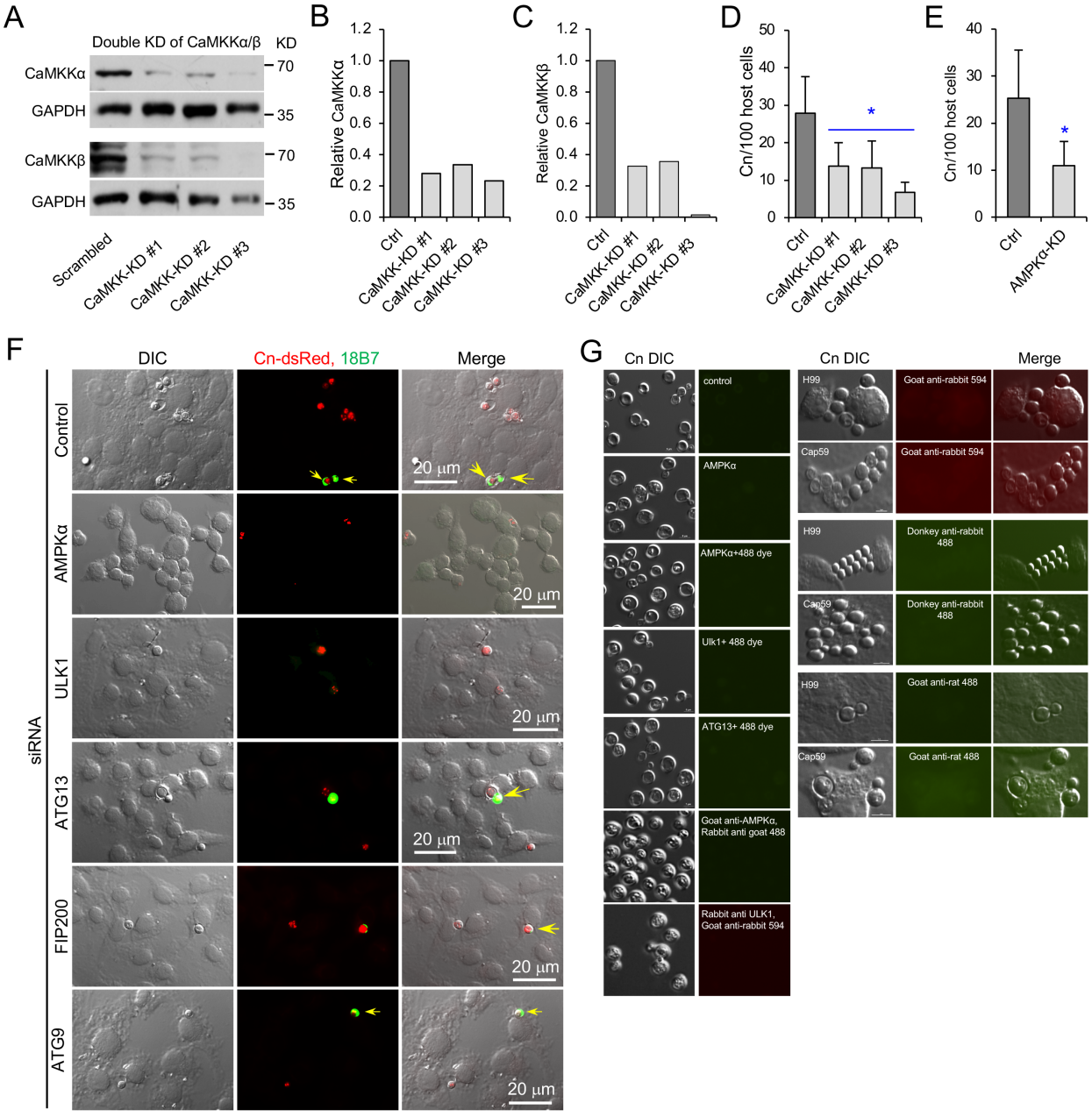
A
Double KD of CaMKKα/β
KD
CaMKKα
GAPDH
CaMKKβ
GAPDH
70
35
70
35
Scrambled
CaMKK-KD #1
CaMKK-KD #2
CaMKK-KD #3
B
Relative CaMKKα
C
Relative CaMKKβ
D
Cn/100 host cells
E
Cn/100 host cells
Ctrl
AMPKα-KD
F
DIC
Cn-dsRed, 18B7
Merge
siRNA
Control
AMPKα
ULK1
ATG13
FIP200
ATG9
20 μm
G
Cn DIC
control
AMPKα
AMPKα+488 dye
Ulk1+ 488 dye
ATG13+ 488 dye
Goat anti-AMPKα, Rabbit anti goat 488
Rabbit anti ULK1, Goat anti-rabbit 594
Cn DIC
Merge
H99
Cap59
Goat anti-rabbit 594
Donkey anti-rabbit 488
Goat anti-rat 488

Figure S5. Components in the CaMKK-AMPK-ULK1 signal axis play important roles in Cn internalization (Related to Figure 4).

(A) Immunoblotting assay to test the depletion of CaMKKα/β protein level by the shRNA approach.

(B, C) Relative protein expression levels of CaMKKα (B) or CaMKKβ (C) in RAW macrophages transfected with scrambled or CaMKKα/β shRNAs. Data from a representative experiment shown in (A). Ctrl: control.

(D, E) Depletion of host cell CaMKKα/β (D) or AMPKα (E) reduces Cn internalization determined by immunofluorescence microscopy assay. Data represent the means ± SEM from three independent experiments. *: significance at $p < 0.05$.

(F) Depletion of host cell AMPKα and AIC components reduces Cn internalization as determined using an immunofluorescence microscopy assay. Cn cells with green fluorescence represent incompletely internalized or extracellular Cn cells. Images from a representative experiment of three independent experiments.

(G) Cn cells harvested from infected host cells (leaf panel) or during host infection (right panel) do not display cross activities with the primary or secondary antibodies used in this work.

Table S1. shRNAs and PCR primers used in this study (Related to Figure 4, Figure S1, and Figure S4)

shRNA ID	Sequence (5'-3')	References
shCaMKKα 1	GGAAGTGCCCGTTCATTGATT	This study
shCaMKKα 2	TCAATGGCTGAGGTGAGGCAC	This study
shCaMKKβ1	GGTGCTGTCCAAAAAGAAA	This study
shCaMKKβ2	TTGCGTAATAAGTATTGTCAT	This study
shFIP200	GAGAGAACTTGTTGAGAAA	Pandey et al., 2017
	ACATGAAGGCTCAGAGAAA	ditto
shUlk1	GAGCAAGAGCACACGGAA A	ditto
	AGACTCCTGTGACACAGAT	ditto
shAtg13	GAGAAGAATGTCCGAGAAT	ditto
	ACAGGAAGGACTTGGACAA	ditto
shPrkaa1	TGAATTAAACCCACAGAAA	ditto
	GGTCATCAGTACACCATCT	ditto
shPrkab1	TGAACAAGGACACGGGCAT	ditto
	GCACGACCTGGAAGCGAAT	ditto
Scramble 1	ATTGTATGCGATCGCAGAC	ditto
Scramble 2	CACCAGCATCTGATCTAGA	ditto
Ulk1-F1	ACTGCGGCCGCatggattacaaggatgacgatgacaagatggag ccgggccgcggcggc	ditto
Ulk1-r1	GAAGAATTCtcaggcatagacaccactcag	ditto
ULK1-F2	GATCTGGATCCGGAGTCGACGGAGCGGCCGCatggatta caagga	ditto
Ulk1-R2	AGCGCCTCCCCTACCCGGTAGAATTCtcaggcatagaca ccactc	ditto
Atg13-F1	ACTAGATCTATGTACCCATACGATGTTCCAGATTACGCT ATGGAAACTGAACTCAGCTCC	ditto
Atg13-R1	GAACTCGAGTTACTGCAGGGTTTCCACAAA	ditto
Atg13-F2	ACTCCTTCTCTAGGCGCCGGAATTAGATCTATGTACCCA TACGAT	ditto
Atg13-R2	ACCCGGTAGAATTCGTTAACCTCGAGttactgcagggtt tccaca	ditto
Prkaa1-F1	ACTGCGGCCGCATGGTGAGCAAGGGCGAGGAGCTGTTCA	ditto
Prkaa1-R1	GAAGAATTCTTACTGTGCAAGAATTTTAAT	ditto
Prkaa1-F2	GATCTGGATCCGGAGTCGACGGAGCGGCCGCATGGTGAG CAAGGG	ditto
Prkaa1-R2	AGCGCCTCCCCTACCCGGTAGAATTCttactgtgcaaga atttta	ditto

Supplemental References

Barhoumi, R., Burghardt, R.C., Qian, Y., and Tiffany-Castiglioni, E. (2007). Effects of propofol on intracellular Ca2+ homeostasis in human astrocytoma cells. Brain Res *1145*, 11-18.

Campeau, E., Ruhl, V.E., Rodier, F., Smith, C.L., Rahmberg, B.L., Fuss, J.O., Campisi, J., Yaswen, P., Cooper, P.K., and Kaufman, P.D. (2009). A versatile viral system for expression and depletion of proteins in mammalian cells. PloS one *4*.

Gee, K.R., Brown, K., Chen, W.U., Bishop-Stewart, J., Gray, D., and Johnson, I. (2000). Chemical and physiological characterization of fluo-4 Ca2+-indicator dyes. Cell calcium *27*, 97-106.

Irving, A.T., Mimuro, H., Kufer, T.A., Lo, C., Wheeler, R., Turner, L.J., Thomas, B.J., Malosse, C., Gantier, M.P., Casillas, L.N.*, et al.* (2014). The immune receptor NOD1 and kinase RIP2 interact with bacterial peptidoglycan on early endosomes to promote autophagy and inflammatory signaling. Cell host & microbe *15*, 623-635.

Pandey, A., Ding, S.L., Qin, Q.M., Gupta, R., Gomez, G., Lin, F., Feng, X., Fachini da Costa, L., Chaki, S.P., Katepalli, M.*, et al.* (2017). Global Reprogramming of Host Kinase Signaling in Response to Fungal Infection. Cell host & microbe *21*, 637-649 e636.

Pandey, A., Lin, F., Cabello, A.L., da Costa, L.F., Feng, X., Feng, H.Q., Zhang, M.Z., Iwawaki, T., Rice-Ficht, A., Ficht, T.A.*, et al.* (2018). Activation of Host IRE1alpha-Dependent Signaling Axis Contributes the Intracellular Parasitism of Brucella melitensis. Front Cell Infect Microbiol *8*, 103.

Qin, Q.M., Luo, J., Lin, X., Pei, J., Li, L., Ficht, T.A., and de Figueiredo, P. (2011). Functional analysis of host factors that mediate the intracellular lifestyle of Cryptococcus neoformans. PLoS Pathog *7*, e1002078.

Qin, Q.M., Pei, J., Ancona, V., Shaw, B.D., Ficht, T.A., and de Figueiredo, P. (2008). RNAi screen of endoplasmic reticulum-associated host factors reveals a role for IRE1alpha in supporting Brucella replication. PLoS Pathog *4*, e1000110.

Sag, D., Carling, D., Stout, R.D., and Suttles, J. (2008). Adenosine 5'-monophosphate-activated protein kinase promotes macrophage polarization to an anti-inflammatory functional phenotype. Journal of immunology *181*, 8633-8641.

Wang, Y., Wang, K., Masso-Silva, J.A., Rivera, A., and Xue, C. (2019). A Heat-Killed Cryptococcus Mutant Strain Induces Host Protection against Multiple Invasive Mycoses in a Murine Vaccine Model. mBio *10*.

Wolf, A., Akrap, N., Marg, B., Galliardt, H., Heiligentag, M., Humpert, F., Sauer, M., Kaltschmidt, B., Kaltschmidt, C., and Seidel, T. (2013). Elements of transcriptional machinery are compatible among plants and mammals. PLoS One *8*, e53737.